JOURNAL OF CHEMICAL & ENGINEERING DATA

Article

pubs.acs.org/jced

Viscosity Measurements of Endothermic Hydrocarbon Fuel from (298 to 788) K under Supercritical Pressure Conditions

H. W. Deng,[†] C. B. Zhang,*[,†,‡] G. Q. Xu,[†] B. Zhang,[†] Z. Tao,[†] and K. Zhu[†]

[†]National Key Laboratory of Science and Technology on Aero-Engine Aero-Thermodynamics School of Jet Propulsion, Beijing University of Aeronautics and Astronautics, Beijing, 100191, P. R. China

[‡]Xi'an Aerospace Propulsion Institute, Xi'an, 710100, P. R. China

ABSTRACT: The viscosity of a typical endothermic hydrocarbon fuel (RP-3) at critical and supercritical conditions is measured using a novel viscosity measurement method by expanding the classical capillary method, and it can be applied to the viscosity measurement of single phase flow, including supercritical fluids. The measurement covers the temperature range of (298 to 788) K under pressures from (2.33 to 5) MPa. The uncertainty of the measurement is within ± (2.14 to 6.42) % (k = 2) according to error analysis. The results are fitted as polynomials to analyze deviations. Out of 219 points, 205 points are within the ± 5 % error band, which is 93.61 %. For all values, the average absolute deviation (AAD) is 2.01 %; the maximum absolute deviation (MAD) appears near the critical point, and the value is 8.83 %.

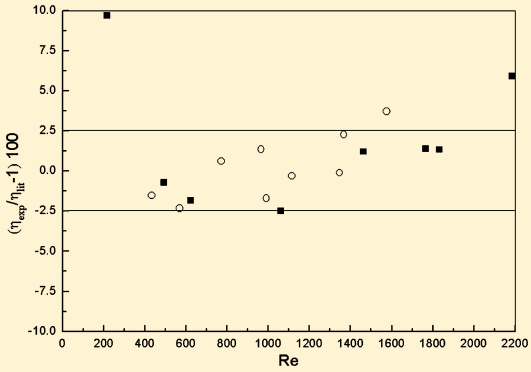

INTRODUCTION

As flight speeds increase to the high supersonic and hypersonic regime, the temperature of the ram air taken on the board of the vehicles becomes too high to cool the structure. Therefore, it is necessary to utilize fuel as the primary coolant. Fuel-cooled aircraft thermal management systems have been widely used with a minimum weight penalty and technical risk.[1] With regard to the needs of the advanced gas turbine engines, the thermophysics properties of fuel are required to be made clear for the sake of safe application. The database for properties of the fuel such as vapor pressure, specific heat, density, viscosity, surface tension, and critical parameters play an essential part in predicting the performance of the components and shortening the design cycle of the engines.[2] For Newtonian fluids, the velocity of the fluid is inversely proportional to its viscosity. Viscosity, therefore, plays a very important role in a wide range of engineering disciplines as well as in determining different fluid properties.

The viscosity of hydrocarbon mixtures is commonly measured by rolling ball viscometer, falling-body viscometer, capillary tube viscometer, and vibrating wire-viscometer. By using the rolling ball viscometer, the viscosities of normal alkanes and their mixtures were measured at 293 K by Dandekar et al.[3] Zéberg-Mikkelsen et al.[4] measured the viscosities of 13 ternary mixtures composed of methylcyclohexane + *cis*-decalin + 2,2,4,4,6,8,8-heptamethylnonane from (293.15 to 343.15) K and up to 100 MPa by using a falling-body viscometer and a classical capillary viscometer. The capillary tube viscometer, which is used as the prescriptive method at room temperature, is simple and very precise in a relatively wide viscosity range. But its application is limited for high temperature and high pressure conditions due to the problems in the use of refractory materials for apparatus and the difficulty of detecting a meniscus.[4,5] Recently, the vibrating-wire viscometer is widely used to measure the viscosities of S20,[6] gaseous propane,[7] and ethane.[8] However, the existing methods for viscosity measurement of supercritical pressure fluids are difficult to use because the range of the viscosity of fluid is too wide from low to high temperatures.

As an extension of our previous studies on the measurement of the density of a typical endothermic hydrocarbon fuel (RP-3),[9] we now present a novel viscosity measurement method for a single phase fluid by expanding the capillary method. By using this method, the viscosities of (RP-3) at supercritical conditions are measured. This paper is organized as follows: First, the experimental apparatus and procedures are described in the Experimental Section. Then the validity of the method is verified, and the viscosities of RP-3 under supercritical conditions are measured in the Results and Discussion section. Finally, a conclusion with some major findings of this paper is reached in the Conclusion section.

EXPERIMENTAL SECTION

Materials. A typical jet fuel RP-3 is used here. The critical point of RP-3 is (T_c = 645.04 K, P_c = 2.33 MPa) which is identified by a critical opalescence phenomenon in our previous work.[10] Composition analysis by using GC6890-MS5975 shows that RP-3 consists of 52.44 % alkanes, 7.64 % alkenes, 18.53 % benzenes, 15.54 % cycloalkanes, 4.39 % naphthalenes, and 1.46 % other. Note that the detailed compositions of RP-3 were

Received: August 10, 2011
Accepted: January 14, 2012
Published: January 30, 2012

reported in our previous work.[9] Water used during this process is double-distilled, and the certified mole purity of nitrogen used in this work is 99.2 %.

Experimental System. A detailed description of the experimental system has been given by Deng et al.[9] Hence, a summary of nothing but the essential items of the system is considered necessary here. The experimental system is composed of a preparative system, a measured system, and a reclaimed system. With regards to the preparative system, the fuel is pumped up to 12 MPa by a piston pump (2J-Z 104/16), and its temperature can be preheated up to 830 K by two preheaters. The measured system includes a test section, pressure transducers, temperature transducers, heat preservation system, and data acquisition system. With regard to the reclaimed system, the hot fuel is cooled lower than 310 K by water cooled shell and tube heat exchanger, and then the fuel pressure is released to ambient pressure through a back pressure valve. Water exhausted from heat exchanger is cooled in cooling tower and then collected for recycling.

Experimental Principles. Under the conditions of ideal adiabatic and isothermal conditions and eliminating the local pressure drop, the force balance equation of fluid flow in horizontal smooth tube is:

$$(P_{in} - P_{out})A - \tau\pi dL = 0 \tag{1}$$

where P_{in} and P_{out} represent the inlet and the outlet pressure of the test tube, respectively; d, L, and A stand for the inner diameter, length, and section circulation area of the test tube, respectively; τ is the frictional shear stress between fluid and tube wall, and $\tau = (\lambda/8)\rho U^2$, where λ, ρ, and U represent the friction coefficient, density, and the average velocity, respectively. Then

$$\Delta P_f = \Delta P = P_{in} - P_{out} = \frac{1}{2}\frac{L}{d}\lambda\rho U^2 = \frac{1}{2}\frac{L}{d}\lambda\frac{\dot{m}^2}{\rho A^2} \tag{2}$$

where $\dot{m}$ is the mass flow rate; ΔP and ΔP_f are the total pressure drop and the frictional pressure drop of the test tube, respectively.

For laminar flow, the analytical solution of the friction coefficient λ is:[11]

$$\lambda = \frac{64}{\mathrm{Re}} \tag{3}$$

where $\mathrm{Re} = (\rho U d)/\eta = (4\dot{m})/(\eta\pi d)$ is the Reynolds number and η is the dynamic viscosity of the fluid. According to eqs 1 to 3, the dynamic viscosity of the fluid can be calculated using the following equation:

$$\eta = \frac{\Delta P\pi\rho d^4}{128\dot{m}L} \tag{4}$$

Equation 4 is the principle of the classical capillary tube viscometer obtained by eleminating the local pressure drop, which is, however, inevitable in experiments. Connections in pipeline, the change of circulation area, deformation of the test tube, and effects of inlet and outlet, and so forth, can cause the local pressure drop. All of them have significant effects on viscosity measurements. Therefore, it is necessary to take some measures to avoid the local pressure drop.

Hence, the long and short tube measurement method is used in this work as follows:

$$\Delta P_{short} = \Delta P_{f,short} + \Delta P_{local,short}$$
$$\Delta P_{long} = \Delta P_{f,long} + \Delta P_{local,long} \tag{5}$$

where ΔP_{short}, $\Delta P_{f,short}$, and $\Delta P_{local,short}$ are the total pressure drop, frictional pressure drop, and local pressure drop of the short measurement tube, respectively; ΔP_{long}, $\Delta P_{f,long}$, and $\Delta P_{local,long}$ are the total pressure drop, frictional pressure drop, and local pressure drop of the long measurement tube, respectively.

In these experiments, the total pressure drops of the long and the short measurement tubes are measured simultaneously. Under the same pressure, temperature, mass flow rate, inside diameter of test tubes, and connections in the test section, the local pressure drops of the long and the short measurement tubes are considered as equal. Thus, the frictional pressure drop for the tube with the length of $L = L_{long} - L_{short}$, can be calculated as

$$\Delta P_f = \Delta P_{f,long} - \Delta P_{f,short} = \Delta P_{long} - \Delta P_{short} \tag{6}$$

Hence, eq 4 can be evolved as

$$\eta = \frac{(\Delta P_{long} - \Delta P_{short})\pi\rho d^4}{128\dot{m}(L_{long} - L_{short})} \tag{7}$$

For most of the fluids, dynamic viscosity changes substantially from room temperature to a higher temperature (>500 K), which causes the mass flow rate to change largely at the same Reynolds number. For example, under the same Reynolds number (Re = 1000), inside diameter (d = 1 mm), and pressure (P = 25 MPa) conditions, the mass flow rate of water is 0.883 g·s^{-1} at 288 K, which then changes into 0.082 g·s^{-1} when the temperature of water increases to 800 K. It is too small to measure for most of the mass flowmeters.

To resolve the measurement problem with small mass flow rates at higher temperatures, the Z-type row of tubes is proposed for viscosity measurements. For the row of tubes, the pressure drop of each branch is the same as that of the row of tubes, while the mass flow rate of each branch is symmetrical. Thus, eq 7 is further evolved as

$$\eta = \frac{(\Delta P_{long} - \Delta P_{short})\pi\rho d^4}{128(\dot{m}/n)(L_{long} - L_{short})} \tag{8}$$

where $\dot{m}$ is the total mass flow rate of the row of tubes; n is the number of tubes; d is the average inside diameter of the long and the short row of tubes; L_{long} and L_{short} are the average lengths of the long and the short measurement tubes, respectively.

In the end, the kinetic viscosity ν is identified as

$$\nu = \frac{\eta}{\rho} = \frac{(\Delta P_{long} - \Delta P_{short})\pi d^4}{128(\dot{m}/n)(L_{long} - L_{short})} \tag{9}$$

It can be seen from eqs 1 to 9 that the basic of the theoreical deviation is that the fluid is a Newtonian fluid and homogeneous. Thus, this method can be applied to the viscosity measurement of liquid, gas, and other homogenious fluids including supercritical fluids in a wide range of temperature and pressure.

Test Section. The test section for viscosity measurement is designed according to the experimental principle. The detailed

dx.doi.org/10.1021/je200901y | J. Chem. Eng.Data 2012, 57, 358−365

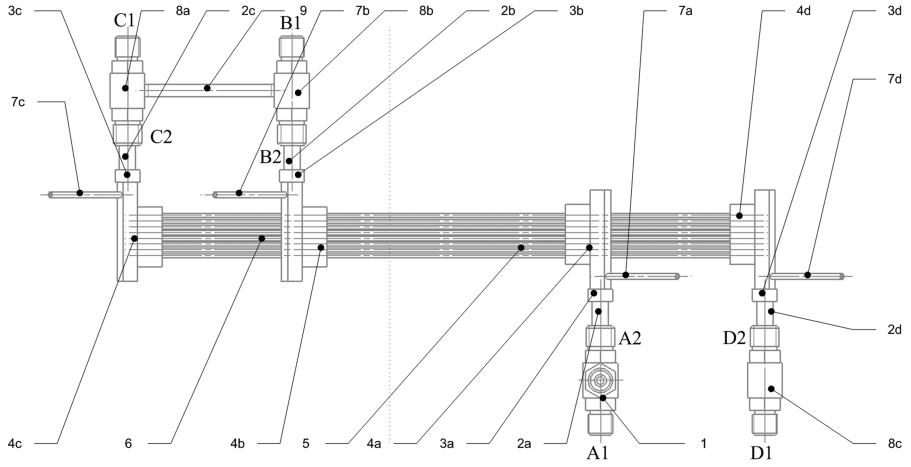

Figure 1. Detailed configuration of the test section (upward view): 1, "+" type connection; 2, stable tube; 3, flow mixer; 4, collecting chamber; 5, short measurement tube; 6, long measurement tube; 7, collecting pipe; 8, T-type connection; 9, leading tube.

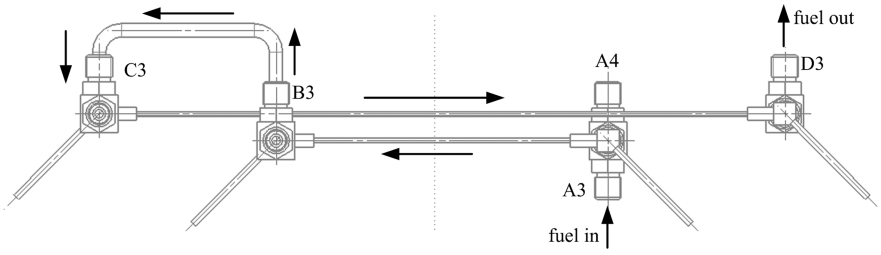

Figure 2. Front view of the test section.

configuration of the test section is shown in Figure 1. Figure 2 is the front view of the test section which is mounted horizontally to avoid the effect of gravity on viscosity measurements. The test section includes a short row of tubes measuring section and a long row of tubes measuring section. Each of them is made up of eight test tubes, two collecting chambers, two stable tubes, two flow mixers, and two collecting pipes. Between the stable tube and the collecting chamber (no. 2 and no. 4 in Figure 1, respectively), a flow mixer (no. 3 in Figure 1) is installed to mix the fluid and ensure homogeneous temperature. On the collecting chamber, there is a pressure port with the diameter of 0.8 mm, the area of which is 2.5 % of the circulation area of the collection chamber. The pressure port is used for differential pressure measurement through a collecting pipe (no. 7 in Figure 1). The short row of tubes measuring section and the long row of tubes measuring section are connected by a leading tube (no. 9 in Figure 1) through two T-type connections (no. 8 in Figure 1). Port A1 of the "+" type connection (no. 1 in Figure 1) and ports B1, C1, and D1 of the T-type connections are used for armored K-type thermocouple connections. Port A4 is used for gauge pressure transducer connection. Ports A3 and D3 are the inlet and outlet of fluid, respectively.

The short measurement tube (no. 5 in Figure 1) and the long measurement tube (no. 6 in Figure 1) are taken from the same tube, whose outside diameter is 2.00 mm. The inside diameter is 1.020 mm, which is measured by a field emission scanning electron microscope (model: CamScan3400). The average inner surface roughness is 0.158 μm, which is measured by the surface morphology measurer (model: Talysurf 5P-120). The test tubes (nos. 5 and 6) and the collecting chamber (no. 4 in Figure 1) are connected by silver brazing, ensuring that no deformation occurs in the measurement tubes. The length (L_{short}, L_{long}) is (140, 300) mm or (300, 500) mm.

Figure 2 also shows the flow direction in the test section. During the experiments, the fluid first flows into the inlet collecting chamber through the "+" type connection, then distributes into each branch of the row of tubes, and finally assembles in the outlet collecting chamber according to Z-type flow. Then, the fluids flow into the long row of tubes measuring section through the leading tube (no. 9). The mass flow rate in each branch of the row of tubes is one out of n of the total mass flow rate, where n is the number of measurement tubes. In fact, the mass flow rate in each branch of the row of tubes is calibrated before the experiments. Compared to the average mass flow rate in each branch, the maximum relative difference is within $\pm$ 3 %, which cannot cause the increase of viscosity calculation error. In addition, the pressure drop of the row of tubes is considered as equal to the pressure drop of each branch of the row of tubes, which is ensured by two techniques: (1) The Z-type row of tubes is designed according to isobaric-differential system design. (2) The area ratio of the circulation area of the collecting chamber and the total circulation area of the row of tubes is greater than 2.

Although the test section is mounted horizontally, the collecting pipe has an angle (45°) to the horizontal level. The nose end of the collecting pipe is downward for the viscosity measurement of liquid (see Figure 2) while it is upward for gas. This step will increase the accuracy of pressure measurements. The viscosity measurement apparatus has been patented (no. 201110136796.X).

In addition, the short row of tubes measuring section and the long row of tubes measuring section are first insulated by heating tape and then insulated by Aspen (an insulating

compound). Moreover, there are two K-type thermocouples with the diameter of 0.1 mm between the short measurement tube and heating tape and three thermocouples between the long measurement tube and heating tape, which are used to monitor and ensure that the wall temperature of the test tube is not higher than the fluid temperature. The heating tapes can ensure that temperature drops in the short row of tubes measuring section and the long row of tubes measuring section are lower than 3 K. Furthermore, the leading tube (no. 9) is heated by power supply to equalize the temperature drop in the short row of tubes measuring section and to ensure that the qualitative temperatures of the short row of tubes measuring section and the long row of tubes measuring section are equal.

It should be stated that the number of the tubes will be increased at higher temperatures to obtain laminar flow under the same measurement error of mass flow rate.

Error Analysis. According to eq 8, the combined standard uncertainty of dynamic viscosity is:

$$\frac{\Delta\eta}{\eta} = \pm[\xi(\Delta P_{long})^2 + \xi(\Delta P_{short})^2 + 16\xi(d)^2 + \xi(\rho)^2 + \xi(L_{long})^2 + \xi(L_{short})^2 + \xi(\dot{m})^2]^{1/2} \quad (10)$$

In this work, the gauge pressure and the differential pressures are measured by a gauge pressure transducer (model 3051CA4, Rosemount) and high-precision differential pressure transducers. For liquid differential pressure measurements, the models are Rosemount 3051CD2A with the measuring range of (0 to 40) kPa and Rosemount 3051CD1A with the measuring range of (0 to 3) kPa; for gas differential pressure measurements, the model is Rosemount 3051S1CD1A with the measuring range of (0 to 6.216) kPa. Each transducer is calibrated by a pressure calibrator supplied by Mesor Ltd., and the maximum measurement uncertainty is found to be within ± 0.065 % of the full range, corresponding to ± (2 to 26) Pa. In our experiments, the differential pressures range from (130 to 21 000) Pa for the long row of tubes measuring section and (80 to 14 000) Pa for the short row of tubes measuring section, corresponding to the relative errors calculated as ± (1.54 to 0.12) % and ± (2.5 to 0.19) %, respectively. The inside diameter is measured by a field emission scanning electron microscope (model: CamScan3400), and the value is very accurate. Considering the asymmetry of the tube, the maximum uncertainty of the inside diameter is within ± 0.2 %. The uncertainty of the density of RP-3 and the mass flow rate have been identified as ± (0.635 to 0.973) % and ± 0.15 %, respectively.[9] The uncertainty of length measurement is ± 0.02 mm, corresponding to the maximum relative uncertainty which is ± 0.014 %. In addition, the accuracy of viscosity and density is influenced by the accuracy of temperature measurement, the uncertainty of which is ± 0.5 K, corresponding to the maximum relative uncertainty which is ± 0.2 %.

Thus, the combined standard uncertainty of dynamic viscosity is calculated as ± (1.07 to 3.21) %. The relative expanded uncertainty of dynamic viscosity measurement is identified as ± (2.14 to 6.42) % (coverage factor k = 2). Similarly, those of the kinetic viscosity are determined as ± (0.87 to 3.06) % and ± (1.74 to 6.12) %, respectively.

RESULTS AND DISCUSSION

Validity and Repeatability. The validity of the method mentioned in this paper is first verified by measuring the dynamic viscosities of water and nitrogen under the pressures of (0.1 and 0.3) MPa, respectively. The temperatures are maintained at 290.32 K for water and 292.35 K for nitrogen.

Figure 3 shows the deviations of ($\eta_{exp}/\eta_{lit} - 1$) versus the Reynolds number, where the subscripts "exp" and "lit" represent experimental and the reference data, respectively. The reference value of water is 1075.11 μPa·s at 290.32 K and 17.575 μPa·s for nitrogen at (292.35 K, 0.3 MPa).[12] It can be seen from Figure 3 that the relative measurement error is within the ± 2.5 % error band when the Reynolds number ranges from 400 to 1400. Thus, the dynamic viscosity in this region is considered as accurate. At a lower Reynolds number, the relative errors of mass flow rate and differential pressure measurements increase, while at a higher Reynolds number, the flow state begins to transit from laminar flow to turbulent flow, which will prove that the analytical solution of frictional coefficient (eq 3) is inapplicable. The results also indicate that the apparatus is capable of obtaining precise data for viscosity measurements in relatively wide viscosity range and it is suitable for viscosity measurements of both liquid and gas.

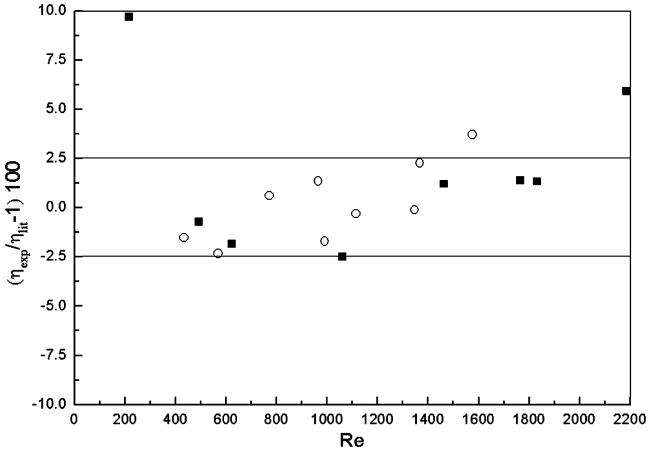

Figure 3. Deviations of ($\eta_{exp}/\eta_{lit} - 1$) versus the Reynolds number. ■, water, 290.32 K, 1 atm; ○, nitrogen, 292.45 K, 3 atm.

The dynamic viscosities of water at different temperatures are then measured according to eq 8 as the repeatability of the experiment method is validated. Table 1 shows two different measurement results of the dynamic viscosity of water under the pressure of 2 MPa which are compared with the reference data.[12] During the experiments, the temperature of water changes from (290 to 400) K, and the Reynolds number is set to be between 800 and 1100. In Table 1, ξ_r is the relative error of viscosity, and the subscript "fit" represents the fitted value of experimental data. It can be concluded from Table 1 that the average absolute deviation (AAD = $(1/\eta)\sum_{i=1}^{n}|((\eta_{exp,i}/\eta_{lit,i}) - 1)|$) and the maximum absolute deviation (MAD = $|((\eta_{exp,i}/\eta_{real,i}) - 1)|$) of dynamic viscosity measurements are found to be about 2.5 % and 3.7 %, respectively. When the two measurement results are fitted using polynomials, the deviations decrease to 2.3 % and 1.1 %. Figure 4 shows the relative error of the fitted experimental dynamic viscosity of water at 2 MPa compared with the reference data.[12] All of the 28 experimental data points are within the ± 4 % error band; after being fitted, all of the data can be within the ± 2.5 % error

dx.doi.org/10.1021/je200901y | J. Chem. Eng.Data 2012, 57, 358–365

Table 1. Relative Error ($\xi_{r,exp}$, $\xi_{r,fit}$) of the Experimental Dynamical Viscosity (η_{exp}) and the Fitted Value (η_{fit}) of Water Compared with the Literature Value (η_{lit}) at 2 MPa

T	η_{lit}[12]	η_{exp}	η_{fit}		
K	μPa·s	μPa·s	μPa·s	$\xi_{r,exp}$	$\xi_{r,fit}$
First Measurement Results					
295.49	945.052	921.021	941.572	−0.0254	−0.0037
304.55	774.206	764.580	770.014	−0.0124	−0.0054
314.21	641.946	634.918	633.194	−0.0109	−0.0136
329.05	500.537	492.020	489.348	−0.0170	−0.0224
337.95	434.438	430.085	429.156	−0.0100	−0.0122
343.98	399.158	395.439	395.722	−0.0093	−0.0086
348.40	376.355	373.034	374.011	−0.0088	−0.0062
358.01	334.325	331.169	332.748	−0.0094	−0.0047
365.49	307.083	303.593	304.702	−0.0114	−0.0078
374.10	280.098	275.958	275.798	−0.0148	−0.0154
381.18	260.517	256.043	254.771	−0.0172	−0.0221
392.25	233.955	230.009	228.615	−0.0169	−0.0228
399.70	218.991	216.683	217.900	−0.0105	−0.0050
Second Measurement Results					
300.41	845.536	820.860	846.662	−0.0292	0.0013
309.17	705.835	706.095	705.624	0.0004	−0.0003
321.54	564.749	560.886	559.323	−0.0068	−0.0096
328.83	499.177	493.602	495.136	−0.0112	−0.0081
335.57	449.951	455.013	446.694	0.0113	−0.0072
346.43	386.200	373.082	385.012	−0.0340	−0.0031
350.11	368.198	355.875	367.569	−0.0335	−0.0017
354.66	347.943	354.538	347.849	0.0190	−0.0003
361.70	320.380	332.169	320.590	0.0368	0.0007
369.02	295.545	300.892	295.529	0.0181	−0.0001
373.24	282.618	273.459	282.339	−0.0324	−0.0010
382.09	258.137	265.494	257.434	0.0285	−0.0027
388.00	243.562	237.357	243.033	−0.0255	−0.0022
394.02	230.183	222.985	230.599	−0.0313	0.0018
399.32	219.689	228.077	221.991	0.0382	0.0105

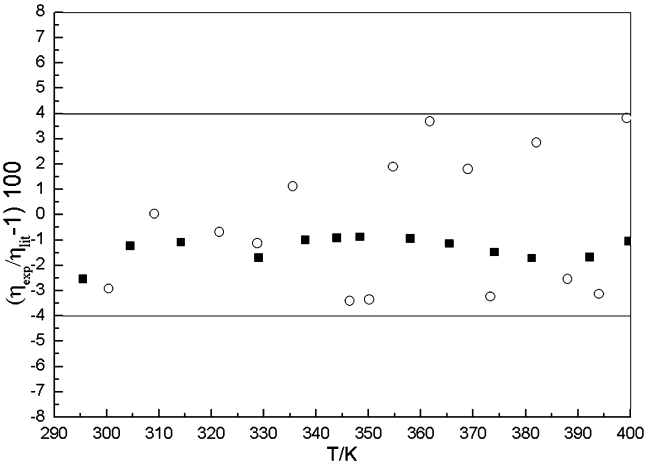

Figure 4. Deviations ($\eta_{exp}/\eta_{lit} - 1$) of the dynamic viscosity of water versus temperature. ○, the first measurement results; ■, the second measurement results.

band, and 24 data points can be within the ± 1.5 % error band, which is 85.7 %.

In this paper, all of the experimental dynamic viscosities at a fixed pressure are fitted according to the following type of sectional polynomials:

$$\eta = \sum_{i=1}^{n} A_i (T/\mathrm{K} - 273.15)^{i-1} \tag{11}$$

where A_i is the temperature polynomial coefficient; n is the number of the polynomial coefficients which is determined by using an F-test.

The experiment results of the dynamical viscosity measurement of water and nitrogen prove that the viscosity measurement method in this study is feasible and accurate. In the following part, the viscosity data of RP-3 at supercritical pressure conditions will be reported, and the effect of temperature and pressure on viscosity will be discussed.

In addition, it can be seen that the measurement error of water is greater than that from the Error Analysis section. The main reason for this may be that, in the Experimental Principles section, it is supposed that the local pressure drop can be totally eliminated by the long and short tube measurement methods, but it is hard to carry out in experiments.

Viscosity of RP-3. The viscosities of RP-3 have been measured at the temperature range of (298 to 788) K and at pressures from (2.33 to 5) MPa. The values of the dynamic and kinetic viscosity data are listed in Table 2.

Figure 5 shows the dynamic viscosity variations of RP-3 versus temperature under different pressure conditions. Like other pure fluids,[12] the dynamic viscosity of RP-3 increases with the increase of pressure especially in critical and pseudocritical regions. Before critical and pseudocritical points, the viscosity of RP-3 exhibits liquid-like properties; hence, the viscosities of RP-3 decrease with the increase of temperature. Beyond these points, it exhibits gas-like properties, and the dynamic viscosities increase with the increase of temperature. In addition, it can be seen from Figure 5 that viscosity variation in the pseudocritical region will be inhibited by the increase of pressure and the temperatures of the minimum value of η increase with the increase of pressure. In fact, the temperatures of the minimum value of η at critical and supercritical pressures are identified as the critical or the pseudocritical temperatures of RP-3. At (2.33, 3, 4, and 5) MPa conditions, the critical and the pseudocritical temperatures of RP-3 are determined as (645.78, 669.83, 701.27, and 716.57) K, respectively. This result is in good agreement with our previous work of the density measurement of RP-3,[9] which is (641.27, 669.88, 698.59, and 710.71) K for (2.34, 3, 4, and 5) MPa, respectively.

Although the accuracy of viscosity measurements has been determined as ± 2.5 % by the fitted experimental values of water in the temperature range of (295 to 400) K at 2 MPa, the measurement error may increase due to the following factors: (1) large density fluctuations occurring at critical point; (2) the relative errors of mass flow rate and differential pressure increase at higher temperatures because the values of which decrease with the increase of temperature. Figure 6 shows the relative error of the fitted experimental dynamic viscosity of RP-3 compared with the experimental data. It can be noticed from Figure 6 that, out of 219 points, 205 points are within the ± 5 % error band, which is 93.61 %. Before critical point, the average absolute deviation (AAD) and the maximum absolute deviation (MAD) between the measured and the fitted dynamic viscosity values are 1.94 % and 7.71 %, respectively; near critical point, (640 to 665) K, AAD = 5.57 % and MAD = 8.83 %, respectively; beyond critical point, AAD = 1.26 % and MAD = 5.01 %, respectively; for all values, AAD = 2.01 %.

dx.doi.org/10.1021/je200901y | J. Chem. Eng.Data 2012, 57, 358−365

Table 2. Fitted Experimental Viscosity (η^a and ν) of RP-3 from T = (298 to 788) K under Supercritical Pressures (P = (2.33 to 5) MPa, P_c = 2.33 MPa)

T	η	ν	T	η	ν	T	η	ν
K	μPa·s	$\mu m^2 \cdot s^{-1}$	K	μPa·s	$\mu m^2 \cdot s^{-1}$	K	μPa·s	$\mu m^2 \cdot s^{-1}$
				P = 2.33 MPa				
300.60	1025.838	1.308	409.46	300.053	0.443	592.34	74.340	0.162
302.11	1001.475	1.279	420.24	272.485	0.409	608.68	61.362	0.14
304.74	960.937	1.231	421.40	269.718	0.405	616.06	54.387	0.129
312.13	858.229	1.109	436.38	237.669	0.366	636.33	30.377	0.096
320.19	763.917	0.997	447.78	217.374	0.341	643.39	20.022	0.082
321.22	753.026	0.984	461.57	196.714	0.316	645.78	16.249	0.077
327.36	693.269	0.913	468.50	187.588	0.306	649.68	16.488	0.103
335.47	626.041	0.833	474.25	180.490	0.297	653.08	16.684	0.139
342.56	576.130	0.773	489.38	163.188	0.277	656.95	16.904	0.146
350.59	527.475	0.715	503.51	148.030	0.258	673.31	17.816	0.177
357.85	489.167	0.67	507.49	143.857	0.253	681.98	18.286	0.193
364.00	459.974	0.635	517.83	133.179	0.239	692.32	18.836	0.214
371.93	425.836	0.595	522.52	128.447	0.233	704.79	19.482	0.239
374.60	415.073	0.582	522.53	128.442	0.233	723.77	20.433	0.278
375.68	410.820	0.577	538.01	113.650	0.214	741.54	21.290	0.316
381.78	387.795	0.549	554.78	98.769	0.194	763.47	22.306	0.365
387.91	366.099	0.523	568.47	89.888	0.183	788.33	23.406	0.421
393.04	349.007	0.502	568.89	89.624	0.182			
394.70	343.650	0.496	579.37	83.034	0.174			
				P = 3 MPa				
301.92	1008.999	1.285	411.13	294.692	0.434	601.48	70.733	0.156
304.69	963.109	1.231	420.27	271.693	0.406	617.78	60.359	0.141
312.00	857.954	1.107	421.55	268.684	0.402	635.30	46.491	0.118
321.41	749.921	0.979	437.22	235.727	0.361	648.47	26.786	0.076
321.91	744.836	0.973	449.64	214.108	0.335	654.97	22.658	0.072
328.07	687.541	0.905	461.68	196.247	0.314	661.72	20.560	0.076
334.97	632.126	0.839	469.67	185.721	0.301	663.69	20.234	0.079
343.14	575.809	0.773	473.14	181.422	0.296	669.83	19.754	0.092
350.95	529.177	0.717	493.00	159.148	0.269	681.70	20.024	0.127
356.71	498.307	0.680	502.90	149.072	0.257	685.41	20.216	0.139
364.04	462.501	0.637	511.17	140.986	0.247	698.39	20.825	0.180
373.03	422.966	0.590	516.86	135.568	0.240	715.65	21.349	0.233
377.12	406.324	0.570	517.53	134.946	0.239	722.85	21.663	0.256
377.55	404.626	0.568	525.61	127.447	0.230	734.77	22.074	0.293
381.90	387.885	0.548	538.41	116.036	0.215	748.80	22.768	0.339
387.27	368.290	0.524	555.06	102.220	0.197	769.68	23.451	0.404
392.14	351.570	0.504	565.77	94.078	0.186	781.74	23.937	0.442
394.31	344.414	0.495	570.39	90.754	0.182			
405.54	310.095	0.453	588.39	78.812	0.166			
				P = 4 MPa				
298.97	1067.380	1.348	410.53	302.633	0.438	595.31	73.864	0.151
302.76	1005.737	1.278	420.49	279.423	0.410	654.91	39.818	0.106
304.01	986.600	1.256	422.30	275.476	0.405	665.40	34.811	0.101
308.40	923.090	1.182	437.86	244.509	0.368	683.44	25.668	0.093
317.57	808.406	1.048	450.01	223.426	0.343	686.79	24.217	0.093
326.23	718.502	0.942	464.60	200.953	0.316	691.52	22.944	0.098
328.79	694.815	0.914	472.69	189.589	0.302	694.08	22.545	0.103
338.28	616.682	0.820	474.65	186.949	0.299	697.98	22.218	0.114
348.25	548.354	0.737	489.98	167.525	0.275	700.07	22.151	0.122
359.85	482.817	0.657	503.42	152.102	0.256	701.27	22.138	0.126
368.08	443.528	0.609	517.64	137.186	0.237	706.50	22.248	0.148
370.21	434.210	0.598	526.85	128.186	0.226	716.15	22.789	0.189
374.67	415.636	0.575	528.66	126.476	0.224	727.84	23.480	0.238
380.23	394.186	0.549	540.38	115.801	0.209	748.67	24.530	0.320
384.92	377.414	0.529	555.64	102.910	0.192	754.63	24.913	0.344
389.53	361.995	0.510	571.00	90.954	0.175	758.44	25.197	0.360
395.48	343.496	0.487	575.26	87.806	0.171	767.33	26.197	0.401

dx.doi.org/10.1021/je200901y | J. Chem. Eng.Data 2012, 57, 358−365

Table 2. continued

T	η	ν	T	η	ν	T	η	ν
K	μPa·s	$\mu m^2 \cdot s^{-1}$	K	μPa·s	$\mu m^2 \cdot s^{-1}$	K	μPa·s	$\mu m^2 \cdot s^{-1}$
				P = 4 MPa				
399.74	331.130	0.472	593.80	74.863	0.153	775.34	27.316	0.441
				P = 5 MPa				
300.34	1076.043	1.358	394.33	357.974	0.503	644.05	54.499	0.123
300.93	1064.800	1.345	410.13	312.293	0.448	650.61	51.482	0.119
304.59	999.033	1.267	423.48	279.079	0.407	667.16	43.933	0.109
311.90	887.083	1.134	427.57	269.766	0.396	682.04	37.135	0.100
320.81	777.759	1.005	438.36	246.834	0.368	690.78	33.101	0.096
327.81	707.799	0.921	452.74	219.743	0.334	691.97	32.549	0.096
328.52	701.352	0.914	463.74	202.121	0.312	698.85	29.334	0.093
328.70	699.726	0.912	474.17	188.980	0.297	706.27	26.311	0.094
334.64	649.833	0.852	478.20	185.203	0.293	712.05	25.204	0.105
343.17	588.309	0.779	490.05	172.175	0.277	714.24	25.033	0.109
351.77	535.825	0.716	503.25	158.450	0.260	716.57	24.953	0.115
358.39	500.522	0.674	515.49	145.868	0.245	720.26	24.985	0.125
364.05	473.131	0.641	518.49	144.165	0.243	731.23	25.580	0.160
371.94	438.600	0.600	533.62	128.299	0.222	739.20	26.020	0.189
375.46	424.375	0.583	543.61	117.875	0.208	754.17	26.484	0.245
381.20	402.565	0.557	557.43	103.449	0.187	769.42	27.003	0.305
383.68	393.599	0.546	572.21	89.983	0.167	788.33	28.758	0.390
383.76	393.311	0.546	604.39	73.717	0.147			
392.86	362.630	0.509	625.45	63.236	0.134			

[a]Considering the situation that various pressure transducers are used for different temperature regimes, the relative uncertainties ξ_r of η in these experiments are: if $T \leq 480$ K, ξ_r ranges from ± (1.07 to 2.48) %; if 480 K < T and $T/T_{Pc} \leq 1$, ξ_r ranges from ± (1.18 to 3.21) %; if $T/T_{Pc} > 1$, ξ_r ranges from ± (3.21 to 1.52) %.

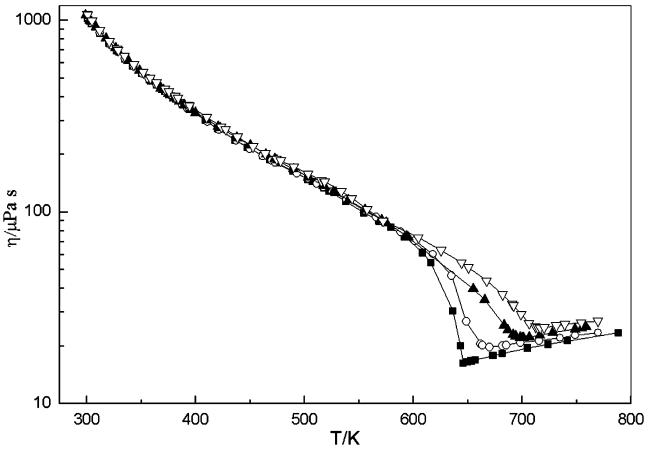

Figure 5. Viscosity variations of RP-3 versus temperature at supercritical pressures. ■, 2.33 MPa; ○, 3 MPa; ▲, 4 MPa; ▽, 5 MPa.

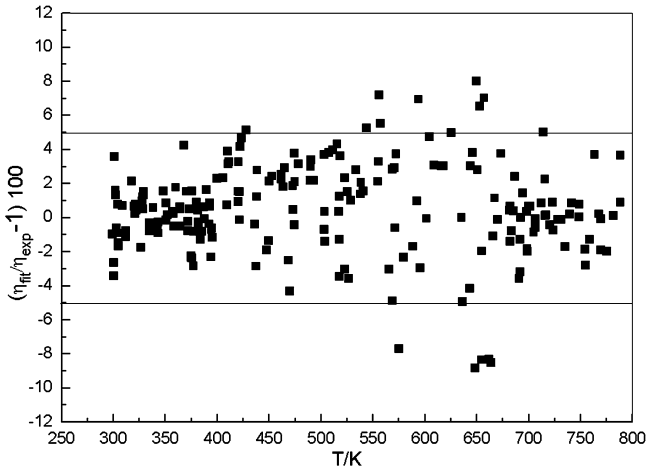

Figure 6. Deviations ($\eta_{fit}/\eta_{exp} - 1$) of the dynamic viscosity of RP-3 versus temperature.

At subcritical pressure, a two-phase flow will be formed when the fluid temperature reaches to its phase transition temperature, which makes it more complex to measure the viscosity of RP-3 at subcritical pressure. This problem will be resolved in our future study.

■ CONCLUSION

A novel viscosity measurement method is proposed based on the momentum conservation equation for the viscosity measurement of single phase flow, including supercritical fluids at high pressure and temperature conditions. The viscosity of a typical endothermic hydrocarbon fuel (RP-3, T_c = 644.05 K, P_c = 2.33 MPa) has been measured at the temperature range of (298 to 788) K under pressures from (2.33 to 5) MPa.

The results of the dynamic viscosities of RP-3 are fitted as polynomials to analyze the average absolute deviation (AAD) and the maximum absolute deviation (MAD). Before the critical point, the average absolute deviation (AAD) and the maximum absolute deviation (MAD) between the measured and fitted dynamic viscosity values are 1.94 % and 7.71 %, respectively; near critical point, (640 to 665) K, AAD = 5.57 % and MAD = 8.83 %, respectively; beyond critical point, AAD = 1.26 % and MAD = 5.01 %, respectively; for all values, AAD = 2.01 %. In addition, viscosity variation in the pseudocritical regions will be inhibited by the increase of pressure, which means the higher the pressure, the larger the viscosity value. Moreover, the critical or the pseudocritical temperatures of RP-3 are identified by the temperatures of the minimum value of η

dx.doi.org/10.1021/je200901y | J. Chem. Eng.Data 2012, 57, 358−365

at supercritical pressures, which are (645.78, 669.83, 701.27, and 716.57) K for (2.33, 3, 4, and 5) MPa, respectively.

AUTHOR INFORMATION

Corresponding Author

*E-mail: zhang_cb@sjp.buaa.edu.cn. Fax: +86-10-82314545.

Funding

This work is funded by the Natural Science Foundation of China under Contract No. 50676005.

ACKNOWLEDGMENTS

The author would like to thank Guo-zhu Liu for his technical support.

REFERENCES

(1) Huang, H.; Spadaccini, L. J.; Sobel, D. R. Fuel-cooled thermal management for advanced aeroengines. *J. Eng. Gas Turb. Power* **2004**, *126*, 284−293.

(2) Fedele, L.; Pernechele, F.; Bobbo, S.; Scattolini, M. Compressed Liquid Density Measurements for 1,1,1,2,3,3,3-Heptafluoropropane (R227ea). *J. Chem. Eng. Data* **2007**, *52*, 1955−1959.

(3) Dandekar, A. Y.; Andersen, S. I.; Stenby, E. H. Measurement of Viscosity of Hydrocarbon Liquids Using a Microviscometer. *J. Chem. Eng. Data* **1998**, *43*, 551−554.

(4) Zéberg-Mikkelsen, C. K.; Barrouhou, M.; Baylaucq, A.; Boned, C. High-Pressure Viscosity and Density Measurements of the Ternary System Methylcyclohexane + cis-Decalin + 2,2,4,4,6,8,8-Heptamethylnonane. *J. Chem. Eng. Data* **2003**, *48*, 1387−1392.

(5) Fukuyama, H.; Waseda, Y. *High-Temperature Measurements of Materials*; Springer: Berlin, 2009; p 18−28.

(6) Kandil, M. E.; Harris, K. R.; Goodwin, A. R. H.; Hsu, K.; Marsh, K. N. Measurement of the Viscosity and Density of a Reference Fluid, with Nominal Viscosity at T = 298 K and p = 0.1 MPa of 29 mPa·s, at Temperatures between (273 and 423) K and Pressures below 275 MPa. *J. Chem. Eng. Data* **2006**, *51*, 2185−2196.

(7) Wilhelm, J. R.; Vogel, E. Viscosity Measurements on Gaseous Propane: Re-evaluation. *J. Chem. Eng. Data* **2011**, *56*, 1722−1729.

(8) Seibt, D.; Voß, K.; Herrmann, S.; Vogel, E.; Hassel, E. Simultaneous Viscosity−Density Measurements on Ethane and Propane over a Wide Range of Temperature and Pressure Including the Near-Critical Region. *J. Chem. Eng. Data* **2011**, *56*, 1476−1493.

(9) Deng, H. W.; Zhang, C. B.; Xu, G. Q.; Tao, Z.; Zhang, B.; Liu, G. Z. Density Measurements of Endothermic Hydrocarbon Fuel at Sub- and Supercritical Conditions. *J. Chem. Eng. Data* **2011**, *56*, 2980−2986.

(10) Deng, H. W.; Zhang, C. B.; Xu, G. Q.; Tao, Z.; Zhu, K.; Wang, Y. J. Visualization experiments of a specific fuel flow through quartz-glass tubes under both sub- and supercritical conditions. **2011**.

(11) Cheng, B. *Fundamentals of Viscous Fluid Dynamics (in Chinese)*; Higher Education Press: Beijing, 2006; p 514.

(12) Lemmon, E. W.; McLinden, M. O.; Huber, M. L. *Reference Fluid Thermodynamic and Transport Properties-REFPROP*, Version 7.1; National Institute of Standards and Technology: Gaithersburg, MD, 2006.